Journal of Power Sources 246 (2014) 767–774

Contents lists available at ScienceDirect

Journal of Power Sources

journal homepage: www.elsevier.com/locate/jpowsour

Reducing capacity fade in vanadium redox flow batteries by altering charging and discharging currents

Ertan Agar [a], A. Benjamin [a], C.R. Dennison [a], D. Chen [b], M.A. Hickner [b,*], E.C. Kumbur [a,**]

[a] Electrochemical Energy Systems Laboratory, Department of Mechanical Engineering and Mechanics, Drexel University, Philadelphia, PA 19104, USA
[b] Department of Materials Science and Engineering, The Pennsylvania State University, University Park, PA 16802, USA

HIGHLIGHTS

- Asymmetric current operation is explored as a technique to reduce capacity loss.
- Diffusion-dominated and convection-dominated membranes.
- Capacity loss of a VRFB is found to decrease with increasing charging current.
- The decrease in capacity loss is greater for the diffusion-dominated membrane.
- Voltage efficiency is found to decrease with an increase in the charging current.

ARTICLE INFO

Article history:
Received 8 May 2013
Received in revised form
27 July 2013
Accepted 5 August 2013
Available online 15 August 2013

Keywords:
Asymmetric current
Capacity fade
Crossover
Energy storage
Membrane
Vanadium flow battery

ABSTRACT

In this study, the operation of a vanadium redox flow battery (VRFB) under asymmetric current conditions (i.e., different current densities during charge and discharge) was investigated as a technique to reduce its capacity loss. Two different membrane types (a convection-dominated membrane and a diffusion-dominated membrane) were analyzed. In these analyses, the charging current density was varied while the discharging current was held constant. For both membranes, it was found that increasing the charging current decreases the net convective crossover of vanadium ions, which reduces the capacity loss of the battery. When the tested membranes were compared, the improvement in capacity retention was found to be larger for the diffusion-dominated membrane (12.4%) as compared to the convection-dominated membrane (7.1%). The higher capacity retention in the diffusion-dominated membrane was attributed to the reduction in the cycling time (and hence, suppressed contribution of diffusion) due to the increased charging current. While asymmetric current operation helps reduce capacity loss, it comes at the expense of a reduction in the voltage efficiencies. Increasing the charging current was found to increase the ohmic losses, which lead to a decrease of 6% and 4.3% in the voltage efficiencies of the convection-dominated and diffusion-dominated membranes, respectively.

1. Introduction

Vanadium redox flow batteries (VRFBs) hold great promise for use in grid-scale energy storage due to their flexible design and ability to efficiently store large amounts of energy. Unlike conventional electrochemical systems (e.g., closed-cell batteries and supercapacitors), VRFBs have a unique system architecture which allows them to decouple energy storage capacity from power output [1–5]. Although this architecture offers a number of key advantages, one major issue that hinders the long-term performance of these systems is the loss of available capacity over time. Typically, VRFBs experience significant capacity fade during cycling, which occurs primarily due to the undesired transport of vanadium ions through the membrane (known as 'crossover'). Species crossover during operation initiates side reactions which reduce the system capacity, lower the device voltage, and increase the operating cost [6].

One main approach to alleviate the crossover problem in these systems is to employ a membrane that has high ion selectivity for ion conduction versus vanadium crossover. To date, a majority of the studies in this field have been largely focused on exploring new membranes that can effectively suppress vanadium crossover while providing reasonable proton conductivity. Various types of membranes, including: proton exchange membranes (PEMs) [7,8], anion exchange membranes [9–11], nanoporous membranes [12] and

* Corresponding author. Tel.: +1 814 867 1847; fax: +1 814 865 2917.
** Corresponding author. Tel.: +1 215 895 5871; fax: +1 215 895 1478.
E-mail addresses: hickner@matse.psu.edu (M.A. Hickner), eck32@drexel.edu (E.C. Kumbur).

0378-7753/$ – see front matter © 2013 Elsevier B.V. All rights reserved.
http://dx.doi.org/10.1016/j.jpowsour.2013.08.023

amphoteric membranes [13,14] have been investigated. While significant progress has been achieved, one major issue limiting the implementation of these membranes is the conductivity/permeability trade-off. In most cases, raising the conductivity of the membrane results in an increase in the vanadium permeability, and vice versa. For instance, increasing the ion exchange capacity improves the proton conductivity; however this improvement often results in an increase in vanadium permeability and water uptake, which increases the crossover [15]. Although with the help of recent efforts, significant advances with regards to performance and capacity fade have been achieved with new membranes as compared to Nafion® (which has been widely accepted as a benchmark membrane for VRFBs), the performance trade-off between conductivity and vanadium permeability in these systems is not well understood at present. The lack of a breakthrough in the conductivity/permeability trade-off is largely due to the lack of understanding of the multi-ionic transport mechanisms and how they are related to the membrane properties. Studies are still underway to better understand this trade-off and explore new membranes that are inexpensive and possess the desired performance characteristics required for long-term VRFB operation.

In addition to tailoring membrane properties, our recent studies [16–18] indicate that one potential approach to reduce the crossover during VRFB operation is altering the operating conditions (e.g., flow type, flow rate) to take advantage of the membrane properties. The idea behind this approach is that by adjusting the operating conditions, it is possible to minimize the driving forces that are responsible for species crossover in the membrane. In our previous studies [16–18], we investigated the transport of vanadium species (V^{2+}, V^{3+}, V^{4+}, V^{5+}) through the membrane as a result of diffusion, convection, and migration. For diffusion-dominated membranes such as Nafion®, we observed that osmotic convection (which occurs due to the difference in viscosities of the electrolytes in positive and negative half-cell giving rise to a pressure gradient across the membrane) has a significant effect on the magnitude and direction of net crossover flux [16]. Accordingly, it was shown that by controlling the pressure gradient across the membrane, the net osmotic convection in a charge/discharge cycle can be minimized, and the net species crossover (and thus capacity fade) can be significantly reduced [17]. This was also experimentally observed in Ref. [19]. Similarly, in a more recent study [18], we compared the species transport mechanisms governing capacity loss in Nafion® 117 and sulfonated Radel (s-Radel) membranes [6]. The goal of this study was to quantify how the differences in key membrane properties affect the dominance of specific species transport mechanisms within the membrane. When compared to Nafion®, s-Radel (composed of post-sulfonated polyphenylsulfone resin – Radel) has been shown to possess superior ion selectivity, high coulombic efficiency, and low capacity fade rate (almost half that of Nafion®) [6]. Our analysis indicated that the transport of vanadium ions across s-Radel is primarily dominated by electro-osmotic convection, which depends on the magnitude and direction of the current [18]. Accordingly, it was suggested that varying the applied current during charging and discharging (i.e., using different current during charge and discharge) can potentially balance the convective crossover (osmosis and electro-osmotic convection) during cycling, which would reduce the capacity fade.

Motivated by the findings in our previous work, in this study, we further explored the effectiveness of altering the charge and discharge current as a potential technique to reduce the capacity loss in VRFBs. Two types of membranes, namely a diffusion-dominated and a convection-dominated membrane, were investigated to assess the effectiveness of the proposed technique with respect to membrane type/properties. Analyses were conducted by using an experimentally-validated VRFB model that was developed by our group [16]. Several studies, including the long-term cycling performance under symmetric (i.e., same current during charge/discharge) and asymmetric current operations (i.e., different currents during charging and discharging) were performed for these two membrane types. The changes in specific transport modes and resulting crossover with respect to tested operating conditions were quantified and linked to the membrane properties to measure the effectiveness of the approach and provide guidance for future optimization efforts.

Table 1
Side reactions incorporated at membrane|electrolyte interface in the model due to crossover [20].

Mobile species[a]	Reaction location	Side reaction
VO^{2+}	Negative half-cell	$VO^{2+} + V^{2+} + 2H^{+} \rightarrow 2V^{3+} + H_2O$
VO_2^{+}	Negative half-cell	$VO_2^{+} + 2V^{2+} + 4H^{+} \rightarrow 3V^{3+} + 2H_2O$
V^{2+}	Positive half-cell	$V^{2+} + 2VO_2^{+} + 2H^{+} \rightarrow 3VO^{2+} + H_2O$
V^{3+}	Positive half-cell	$V^{3+} + VO_2^{+} \rightarrow 2VO^{2+}$

[a] Indicates species which crosses over and initiates the side reaction.

2. Model formulation and method of approach

2.1. Assumptions and governing equations

The proposed asymmetric current operation technique was evaluated using a 2-D, transient, isothermal VRFB model previously developed by the authors [16]. The model has five domains (i.e., positive/negative current collector plates, negative/positive electrode, and membrane) and was constructed based on the assumptions that i) the electrolyte flow is incompressible, ii) the mass and charge transfer properties of the electrode, electrolyte and membrane (i.e., diffusion coefficients, resistivity, etc.) are isotropic, iii) hydrogen and oxygen evolution are neglected, iv) all domains in the cell are isothermal and v) variations in concentration, potential, and pressure in the z-direction are neglected (i.e., 2-dimensional). Detailed information about this model, including governing equations, boundary and initial conditions for each domain, can be found in our previous studies [16–18]. However, for the sake of the readers, a brief description regarding how the species transport is modeled in the membrane (the key domain for the current study) is provided below.

The model incorporates the transport of all vanadium species, water, protons and sulfate ions across the membrane as a result of convection, diffusion, and migration. The transport of species through the electrodes and membrane is modeled using the Nernst–Plank equation:

$$\vec{N}_i^{m} = -D_i^{m}\nabla c_i^{m} - z_i\frac{F}{RT}D_i^{m}c_i^{m}\nabla\varphi_i^{m} + \vec{v}^{m}c_i^{m} \quad (1)$$

where c_i^{m} is the bulk concentration of species i in the membrane, $\vec{N}_i^{m}$ is the flux of the species i in the membrane, D_i^{m}. is the diffusion coefficient of species i in the membrane, c_i^{m}. is the diffusion coefficient of species i in the membrane, z_i is the valence for species, R is the universal gas constant and T is temperature, F is Faraday's constant, and φ_l is the ionic potential. The velocity term, v is given by an alternate form of Schlogl's equation for describing the convective transport of bulk electrolyte:

$$\vec{v}^{m} = -\frac{\kappa_p}{\mu_w}\nabla p - \frac{\kappa_\varphi}{\mu_w}c_f F\left(\nabla\varphi_l^{m} + \frac{RT\sum z_i D_i^{m}\nabla c_i^{m}}{F\sum z_i^2 D_i^{m}c_i^{m}}\right) \quad (2)$$

where μ_w is the viscosity of bulk electrolyte, κ_p is the electrokinetic permeability and κ_φ is the hydraulic permeability. This equation accounts for i) the osmosis of electrolyte through the membrane as

a result of pressure differences between the half-cells and ii) the electro-osmotic convection caused by the viscous interactions between the fluid and the mobile ions. In addition, the model uses a set of boundary conditions based on Eqs. (3) and (4) for the conservation of flux and current at the electrolyte|membrane interfaces to account for the side reactions (Table 1) [20] associated with crossover, and to capture the variations in the electrolyte volume due to the species crossover and side reactions:

$$\frac{\partial(\varepsilon c_i^m)}{\partial t} + \nabla \cdot \vec{N}_i^m = 0 \quad (3)$$

$$0 = \nabla \cdot \vec{j}_l^m = F \sum z_i \nabla \cdot \vec{N}_i^m \quad (4)$$

where ε is the porosity and j_l is the liquid current density. Another feature of this model is that it accounts for the Donnan potential across the membrane, which enables accurate prediction of the cell potential without using a fitting voltage value [21]. The model was built using COMSOL and validated using in-house performance data [16] and several extended cycling data reported in the literature [6].

2.2. Simulated case studies

In this study, simulations were performed for two different membrane types (i.e., diffusion-dominated and convention-dominated membrane), in which different transport modes dominate species crossover. For the diffusion-dominated membrane, Nafion® 117 was selected as an exemplary membrane for analysis. Nafion® 117 has been extensively studied in other fields and its properties have been well-characterized [22–26] (see Table 2). In addition, Nafion has been used in many VRFB studies [27–33] as a baseline membrane to study device performance. For the convection-dominated membrane, we selected a model membrane (see Table 2) that has properties similar to those found in s-Radel (e.g., much lower diffusivity and higher ion exchange capacity than Nafion®) [6]. The selection of the properties for the convection-dominated membrane was performed based on the findings in our previous reports [18, 34-35]. Our previous work indicates that the transport of vanadium ions due to convection (specifically electro-osmotic convection) is more dominant for the membranes that have large number of fixed acid sites and free ions [18]. With the larger number of fixed charges, more interaction is expected to occur between the charged species within the membrane, which would lead to higher electro-osmotic drag of electrolyte across the membrane [18].

Table 2
Membrane properties and parameters used in the model.

Symbol	Description	Nafion® 117	Convection-dominated membrane
L^m	Membrane thickness (μm)	203 [22]	115
c_f	Fixed acid concentration (mol m^{-3})	1432 [22]	2800
κ_φ	Electrokinetic permeability (m^2)[a]	1.13×10^{-20}	7.533×10^{-21}
κ_p	Hydraulic permeability (m^2)	1.58×10^{-18} [23]	5.27×10^{-19}
D_{II}^m	V (II) membrane diffusion coefficient (m^2 s^{-1})[a]	3.125×10^{-12}	2.0×10^{-13}
D_{III}^m	V (III) membrane diffusion coefficient (m^2 s^{-1})	5.93×10^{-12} [24]	3.80×10^{-13}
D_{IV}^m	V (IV) membrane diffusion coefficient (m^2 s^{-1})	5.0×10^{-12} [24]	3.21×10^{-13}
D_V^m	V (V) membrane diffusion coefficient (m^2 s^{-1})	1.17×10^{-12} [24]	7.5×10^{-14}
$D_{H^+}^m$	H^+ membrane diffusion coefficient (m^2 s^{-1})	3.35×10^{-9} [25]	2.68×10^{-9}
$D_{HSO_4^-}^m$	HSO_4^- membrane diffusion coefficient (m^2 s^{-1})	4×10^{-11} [26]	2×10^{-11}

[a] Fitted parameter.

In terms of simulations, the convection-dominated membrane was simulated at four different charging current densities (e.g., 400 A m^{-2}, 600 A m^{-2}, 800 A m^{-2} and 1000 A m^{-2}), while the discharge current was held constant at 600 A m^{-2} for each case. Similarly, the diffusion-dominated membrane (Nafion® 117) was simulated at a charging current density of 500 A m^{-2} and 1000 A m^{-2} while the discharging current was held constant at 500 A m^{-2}. There are two main reasons why the charging current was varied while the discharging current was kept constant in this study. The first reason is that from an operational perspective, a VRFB is typically considered for use a generator in the electricity market and must satisfy the load, in which it is dispatched to serve, up to the maximum power bid placed by the operator. Thus, the output power of the system is dictated by the demand for electricity, and cannot be actively controlled by the operator to minimize crossover. However, when the system is charging (i.e., acting as a load on the electrical grid), the consumption can be varied at the operator's discretion. For this reason, it is reasonable to consider the charging current as the controllable variable. The second reason is that in our previous study, it was found that crossover appears to occur much more during discharging than charging [18]. Therefore, changing the current during charging would provide more insight with regards to the possibility of balancing the species crossover (and thus reducing overall net crossover) between charging and discharging.

In these simulations, the active area of the flow cell was selected as 10 cm^2. The model was run to simulate charging/discharging for 40 cycles with an electrolyte flow rate of 20 mL min^{-1}. During each cycle, the VRFB was charged and discharged to cutoff voltages of 1.7 V and 1.1 V, which correspond to ~95% and ~10% SOC, respectively.

3. Results and discussion

3.1. Capacity loss for the convection-dominated membrane with respect to asymmetric current operation

Fig. 1 compares the capacity fade for the convection-dominated membrane under four different charging current conditions. As seen in Fig. 1, the capacity loss of the VRFB under all four operating conditions generally follows the same trend. Initially, the loss in capacity is not significant due to very small amount of accumulation of vanadium ions in each half-cell. However, as the VRFB continues to be cycled, the change in capacity is more pronounced due to the build-up of vanadium species in each half-cell. When the tested conditions are compared, it is observed that the change in capacity considerably varies with increasing the charging current from 400 A m^{-2} to 1000 A m^{-2}, which indicates the benefit of operating the VRFB under an asymmetric current condition. As seen in Fig. 1, an improvement of ~ 7.1% in the capacity retention is observed at the end of 40th cycle for 1000C/600D case, as compared to 400C/600D case (C represents charging where *D* represents discharging current density).

To investigate the rationale behind this improvement, the change in the crossover of vanadium ions with respect to the tested conditions was analyzed. Fig. 2 shows a representative analysis of the crossover mechanisms for V^{2+} for the 20th cycle at 50% state of charge (SOC). As the charging current density increases, the diffusive and migrative fluxes do not change substantially. Diffusion is driven by the concentration gradients that exist across the membrane, whereas migration is driven by the potential gradient between the two half-cells. Neither of these parameters (i.e.,

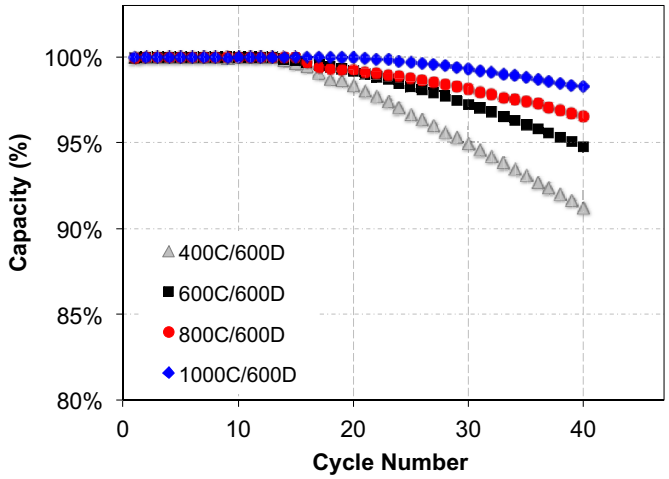

Fig. 1. Capacity loss over 40 cycles for the convection-dominated membrane when operated at 400C/600D (charging at 400 A m^{-2} and discharging at 600 A m^{-2}), 600C/600D, 800C/600D, and 1000C/600D.

concentration and potential gradient) is significantly affected by the increase in the charging current density, therefore the change in diffusive and migrative flux is observed to be very small (almost negligible) for all these tested cases (Fig. 2). On the other hand, the convective flux during charging is observed to increase with the charging current and consequently, the net convective flux over the course of a single cycle decreases as the charging current increases from 400 to 1000 A m^{-2}. It is important to note that V^{2+} ions are not allowed to exist in the positive electrolyte. Accordingly, the observed flux of V^{2+} ions is not from the positive electrolyte, but rather from the membrane itself; this presence of vanadium ions is a direct consequence of the relatively high fixed acid concentration within the membrane. Since convection is the dominant transport mechanism for this type of membrane, a decrease in the net convective flux also contributes to a reduction in the net "total" crossover flux of vanadium ions (Fig. 2).

To further investigate this observation, the change in the flux of individual vanadium species was analyzed. Fig. 3 shows the net crossover flux of each vanadium species (V^{2+}, V^{3+}, V^{4+} and V^{5+}) at 50% SOC for the 20th cycle under the test conditions. Similarly, the net crossover of all species is observed to decrease considerably as the charging current density increases from 400 to 1000 A m^{-2}. The decrease in the net crossover flux of each vanadium ion represents the primary reason for the observed 7.1% improvement in the capacity retention with increasing charging current shown in Fig. 1.

3.2. Dependence of capacity loss on charging current

The simulation results shown in Figs. 2 and 3 suggest that the magnitude and direction of "net" crossover flux for the convection-dominated membrane highly depends on the charging current. In order to quantify this dependency, the convective crossover of the bulk electrolyte was predicted for the tested conditions and is shown in Fig. 4. Fig. 4a, c, and d depict the convective crossover of the bulk electrolyte under asymmetric current conditions, whereas Fig. 4b shows the convective crossover during the symmetric current operation. In each of these cases, osmotic convection is found to occur in the same direction with the same magnitude (for both

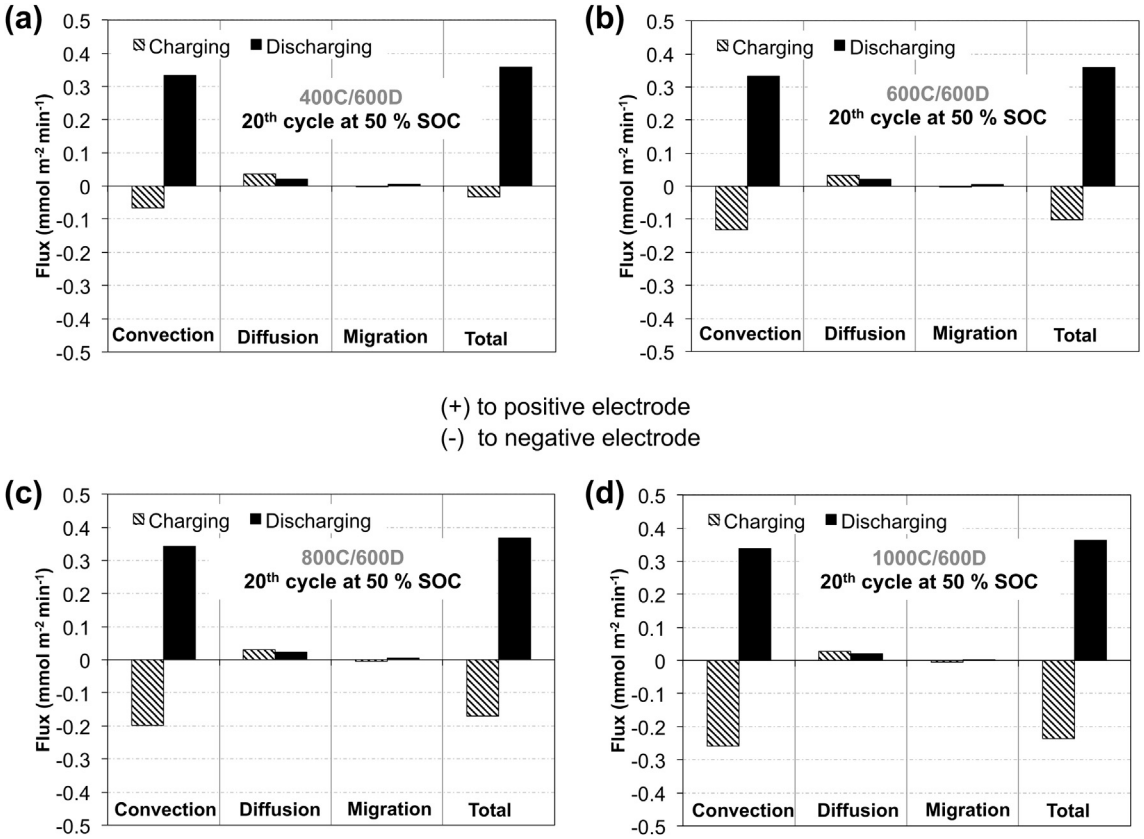

Fig. 2. Crossover flux of V^{2+} ions due to diffusion, convection, and migration (20th Cycle at 50% SOC) when operated at (a) 400C/600D (charging at 400 A m^{-2} and discharging at 600 A m^{-2}); (b) 600C/600D; (c) 800C/600D; (d) 1000C/600D for the convection-dominated membrane.

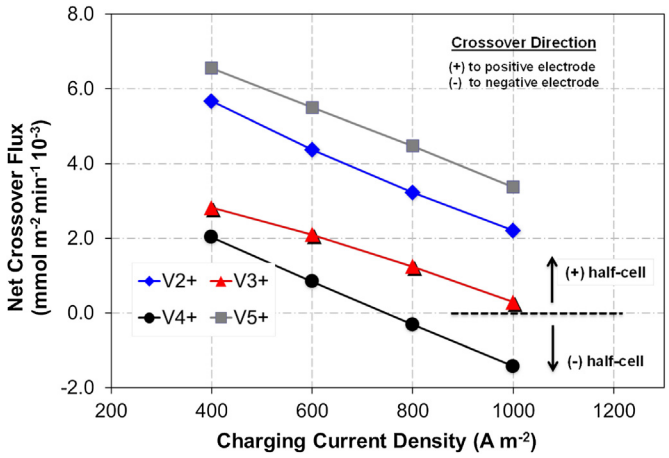

Fig. 3. Net crossover flux of V^{2+}, V^{3+}, V^{4+}, and V^{5+} (20th Cycle at 50% SOC) when operated at 400C/600D (charging at 400 A m^{-2} and discharging at 600 A m^{-2}), 600C/600D, 800C/600D, and 1000C/600D for the convection-dominated membrane.

charging and discharging) irrespective of the charging current. This trend is expected since osmotic convection is driven by the pressure gradient across the membrane, rather than the current. The electro-osmotic convection, on the other hand, appears to be considerably affected by the charging current. Under asymmetric current operation, simulation results indicate that the electro-osmotic convection during charging and discharging is not balanced (e.g., having different magnitudes and directions). As the charging current increases from 400 A m^{-2} to 1000 A m^{-2}, the electro-osmotic convection during "charging" is observed to increase. This increase appears to compensate for the impact of the osmotic crossover, and leads to a decrease in the overall "net" convective flux.

To further investigate this observation, the change in volume of electrolyte in each half-cell was analyzed for all these four conditions. A representative analysis of change in electrolyte volume for 20th cycle is shown in Fig. 5. It is observed that the net rate of vanadium crossover is greater during discharging than charging for all the tested conditions. Furthermore, increasing the charging current density appears to reduce the net change in volume of electrolyte in each half-cell at the end of the cycle. This finding also agrees well with the previous observation of reduced "net" convective crossover with increasing charging current.

It is also important to note that although a significant reduction in capacity fade was observed by operating under asymmetric current conditions, the capacity loss was not entirely eliminated for the convection-dominated membrane. This is due to the contributions of diffusion to the overall crossover of vanadium ions. As shown in Fig. 2, although the effect of convection is significantly minimized with increasing charging current, diffusion (driven by the concentration gradient across the membrane) occurs in the same direction during charging and discharging. As a result, the net contribution of diffusion for each vanadium species, at the end of a single cycle is non-zero, which leads to a small capacity loss in the system. However, it should be noted that as the VRFB is continually cycled, the driving force for diffusion (i.e. the concentration gradient) gradually diminishes over time with the accumulation of an equivalent concentration of vanadium ions in each half-cell.

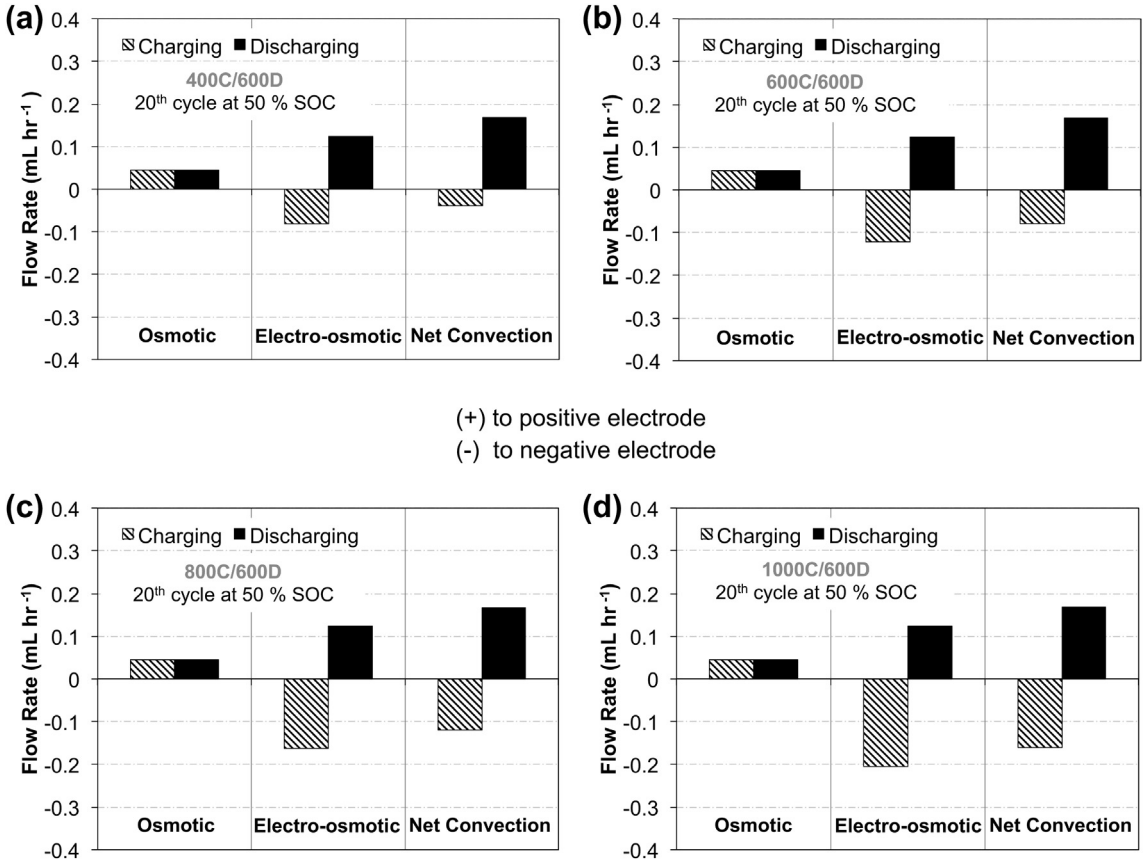

Fig. 4. Convective crossover (osmotic, electro-osmotic, and total) of bulk electrolytes (20th Cycle at 50% SOC) when operated at (a) 400C/600D (charging at 400 A m^{-2} and discharging at 600 A m^{-2}); (b) 600C/600D; (c) 800C/600D; (d) 1000C/600D for the convection-dominated membrane.

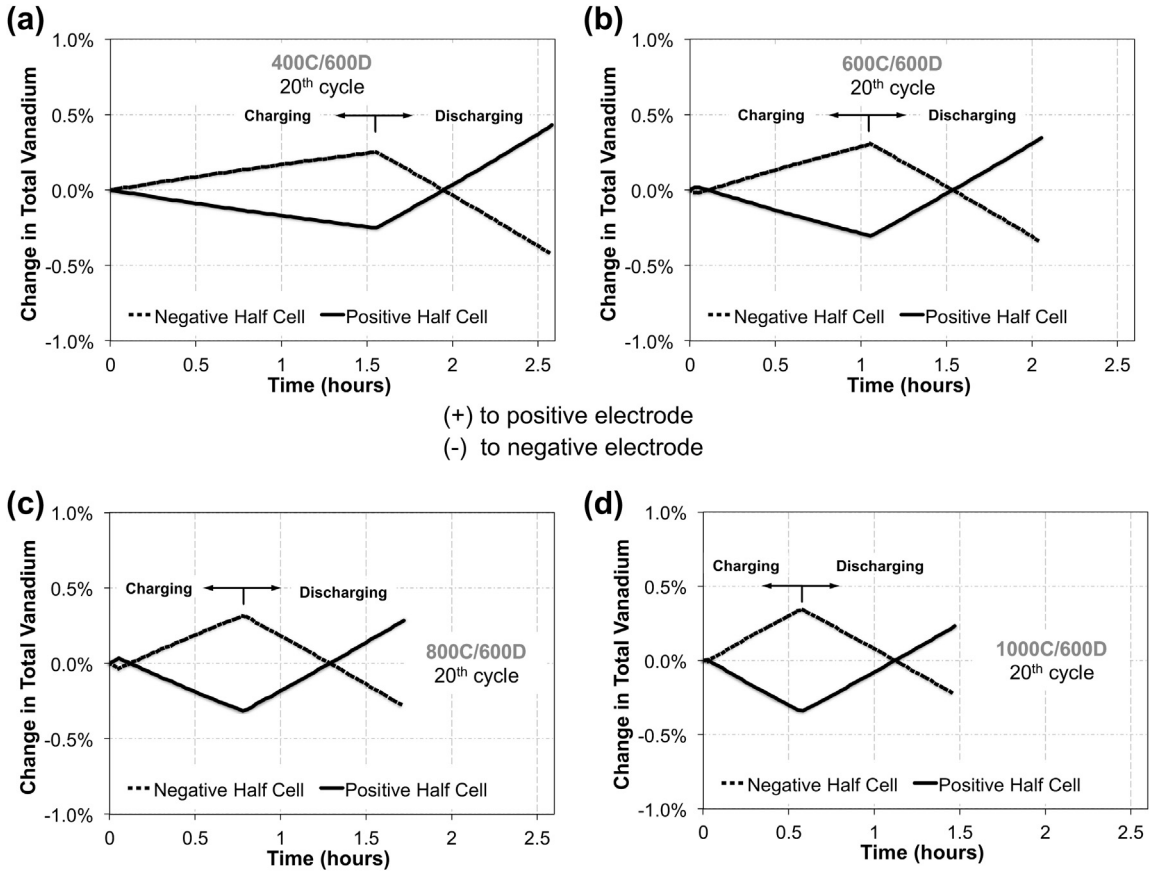

Fig. 5. Change in volume of each half-cell (20th Cycle) operated at (a) 400C/600D (charging at 400 A m^{-2} and discharging at 600 A m^{-2}); (b) 600C/600D; (c) 800C/600D; (d) 1000C/600D for the convection-dominated membrane. Note: The numerical artifacts seen in Fig. 5b and c are believed to be caused by discontinuities in the simulations when switching from charging to discharging and vice versa.

3.3. Voltage efficiencies for the convection-dominated membrane

The simulation results indicate the possibility of reducing the capacity loss for the convection-dominated membrane by running the system under asymmetric current operation (i.e., increasing charging current). In order to determine the efficiency cost of this improvement, the voltage efficiencies of the system under each condition were analyzed. As shown in Fig. 6, increasing the charging current density from 400 A m^{-2} to 1000 A m^{-2} decreased the average voltage efficiency over 40 cycles by ~6%. This reduction in voltage efficiency can be attributed to the increased ohmic losses as a result of increased charging current. Increasing the charging current density increases the rate at which ions flow across the membrane to maintain the electroneutrality in the system. Assuming that the resistance of the membrane stays fairly constant, an increased current across the membrane manifests itself as a higher voltage drop (i.e., ohmic loss), which would adversely impact the voltage efficiencies. The same ohmic behavior occurs in the electrodes and current-collectors as well.

3.4. Capacity loss for the diffusion-dominated membrane (Nafion® 117)

In the second part of this study, Nafion® 117 was simulated in order to investigate the effects of asymmetric current operation on the diffusion-dominated membrane. In these simulations, two different charging current densities (500 A m^{-2} and 1000 A m^{-2}) were simulated, while the discharging current was held constant at 500 A m^{-2}. The simulated charging current densities are representative of the high and low ends of those used in the simulations for the convection-dominated membrane to gauge the impact of asymmetric current operation. In our previous study [18], it was found that under symmetric current condition, the net convective crossover is always greater during discharging than charging due to the dominance of osmotic convection, which occurs in the same direction for both charging and discharging.

Fig. 7 shows the predicted capacity loss and voltage efficiency over 40 cycles for the diffusion-dominated membrane. It is

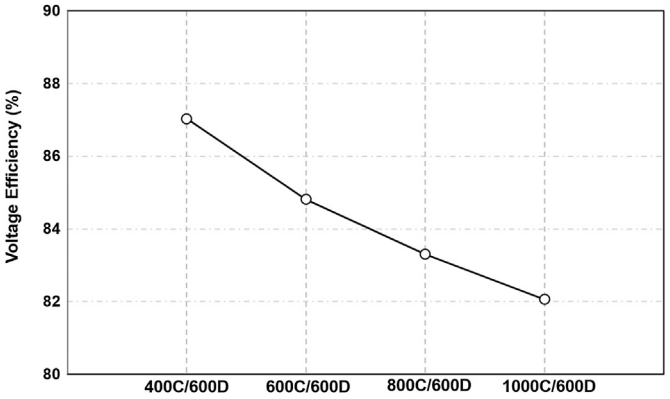

Fig. 6. Average voltage efficiency over 40 cycles when operated at 400C/600D (charging at 400 A m^{-2} and discharging at 600 A m^{-2}), 600C/600D, 800C/600D, and 1000C/600D for the convection-dominated membrane.

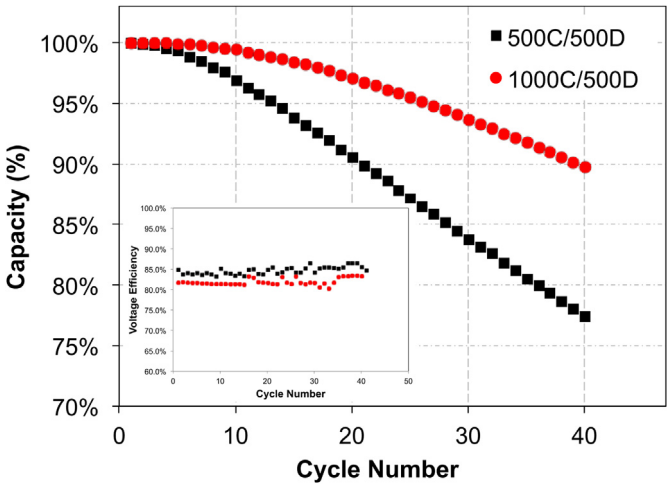

Fig. 7. Capacity loss and voltage efficiency over 40 cycles when operated at 500C/500D (charging at 500 A m^{-2} and discharging at 500 A m^{-2}), and 500C/500D for the diffusion-dominated membrane.

observed that increasing the charging current from 500 to 1000 A m^{-2} decreases the capacity loss by approximately 12.4%. However, the average voltage efficiency over 40 cycles is observed to decrease by ~4.3% due to the increased ohmic losses.

Physical insight into the observed decrease in the capacity fade was obtained by investigating the crossover of active species across the membrane. Figs. 8 and 9 show the crossover flux for all mechanisms (i.e., convection, diffusion and migration), and the convective crossover of the bulk electrolyte under these two operating conditions, respectively. As seen from Fig. 8, the main difference between these two cases is the direction of convection during charging. As the charging current is increased from 500 A m^{-2} to 1000 A m^{-2}, convection during charging changes direction, which leads to a reduction in "net" convection at the end of a full cycle (Fig. 8b). As shown in Fig. 9, this change of direction in convection stems from the increased electro-osmotic drag during charging with increasing charging current. Furthermore, increasing the charging current density increased the magnitude of the electro-osmotic crossover during charging, which compensates for the osmotic crossover and reduces the "net" convective crossover. The decrease in "net" convection leads to a reduction in the total crossover flux, which manifests itself as a reduction in the overall capacity loss of the device.

3.5. Comparison of the convection-dominated vs. the diffusion-dominated membrane

When both membranes are compared, simulation results indicate that operating under asymmetric current conditions can mitigate capacity fade in VRFBs regardless of the membrane type. For both membranes, increasing the charging current density appears to help reduce the net convective crossover of ions, which

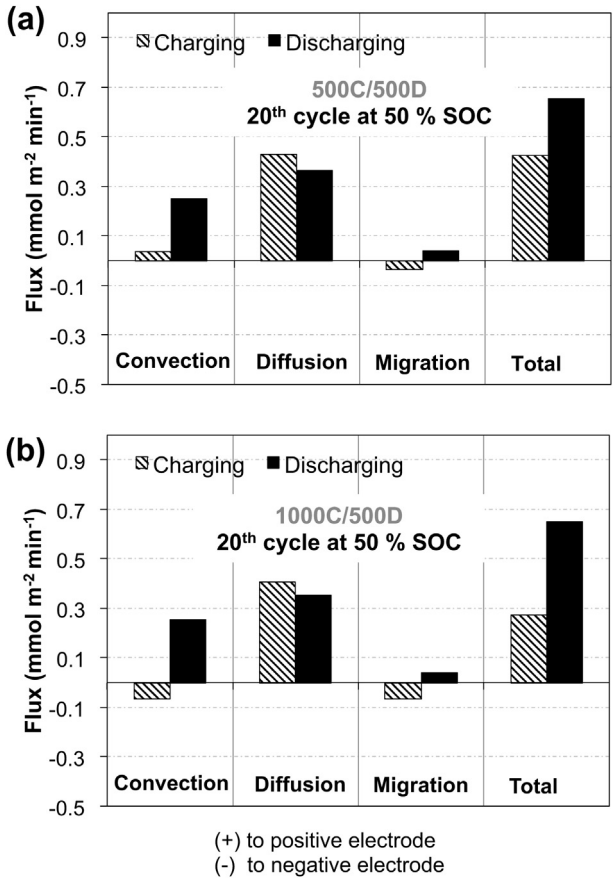

Fig. 8. Crossover flux of V^{2+} ions due to diffusion, convection, and migration (20th Cycle at 50% SOC) when operated at (a) 500C/500D (b) 1000C/500D for the diffusion-dominated membrane.

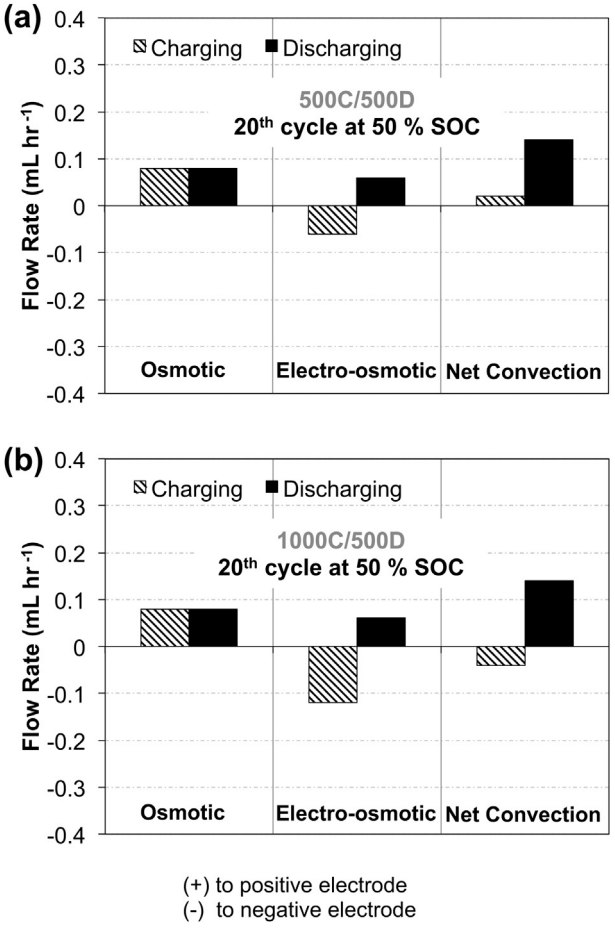

Fig. 9. Convective crossover (osmotic, electro-osmotic, and total) of bulk electrolytes (20th Cycle at 50% SOC) when operated at (a) 500C/500D (b) 1000C/500D for the diffusion-dominated membrane.

diminishes the loss of capacity. However, when the magnitude of the reduction in capacity loss is compared, a more significant reduction in capacity fade is observed for the diffusion-dominated membrane (~12.4%, see Fig. 7), as compared to the convection-dominated membrane (~7.1%, see Fig. 1). This observed discrepancy can be attributed to the reduction in the overall cycle time under asymmetric current operation. For Nafion® 117, the impact of diffusion (i.e., the dominant transport mechanism) is essentially suppressed due to a reduction in the overall cycle time. Increasing the charging current density from 500 A m^{-2} to 1000 A m^{-2} decreased the cycle time by ~33%. Since the concentration gradients for all vanadium species remain relatively constant over 40 cycles, a reduced cycle time translates to a decrease in the crossover of vanadium ions due to diffusion. The convection-dominated membrane, on the other hand, was found to be less sensitive to cycle time since the contribution of diffusion to the overall crossover is relatively smaller. For this type of membrane, the total convective flux (i.e., dominant transport mechanism) depends on other factors besides time (such as, pressure difference across the membrane, current density, etc), which makes it less sensitive to the changes in cycle time.

4. Conclusions

In this study, asymmetric current operation (i.e., different current during charging and discharging) was investigated as a technique for mitigating the capacity fade of a VRFB for both convection-dominated and diffusion-dominated membranes. For both types of membranes, it was found that increasing the charging current density decreases the net convective crossover of the bulk electrolyte, which leads to a reduction in the overall crossover at the end of the cycle. This observation was attributed to the fact that increasing the charging current increases the magnitude of the electro-osmotic convection during charging, which in turn, compensates for the convective crossover due to osmosis. Furthermore, when both membranes are compared, a more significant improvement in capacity retention was observed for the diffusion-dominated membrane because of the fact that diffusion has less time to influence the capacity during a single cycle as a result of increased charging current. On the other hand, the convection-dominated membrane was found to be less affected by similar changes in cycle time, since the impact of diffusion is very small as compared to the convection. While the simulation results indicate that asymmetric current operation offers an opportunity to increase the life span of a VRFB regardless of membrane type, it comes at the expense of reduction in the voltage efficiencies due to the increased ohmic losses.

Along with our previous reports, the findings of this study highlight the importance of intelligent selection of operating conditions on reducing the capacity fade of VRFBs. An optimal solution to capacity fade will probably result when operating conditions are matched to the crossover behavior of the membrane. Developing such operational strategies will compliment advances in membrane development for these systems.

Acknowledgements

The authors would like to thank the support from the Southern Pennsylvania Ben Franklin Commercialization Institute (Grant # 001389-002) and also thank Mr. Kevin W. Knehr for valuable discussion.

References

[1] M. Skyllas-Kazacos, F. Grossmith, J. Electrochem. Soc. 134 (12) (1987) 2950–2953.
[2] M. Skyllas-Kazacos, D. Kasherman, D.R. Hong, M. Kazacos, J. Power Sources 35 (1991) 399–404.
[3] M. Skyllas-Kazacos, Encycl. Electrochem. Power Sources (2009) 444–453.
[4] A.Z. Weber, M.M. Mench, J.P. Meyers, P.N. Ross, J.T. Gostick, Q. Liu, J. Appl. Electrochem. 41 (2011) 1137–1164.
[5] G. Qui, A.S. Joshi, C.R. Dennison, K.W. Knehr, E.C. Kumbur, Y. Sun, Electrochim. Acta 64 (2012) 46–64.
[6] S. Kim, J. Yan, B. Schwenzer, J. Zhang, L. Li, J. Liu, Z. Yang, M.A. Hickner, Electrochem. Commun. 12 (2010) 1650–1653.
[7] W. Wei, H. Zhang, X. Li, Z. Mai, H. Zhang, J. Power Sources 208 (2012) 421–425.
[8] X. Luo, Z. Lu, J. Xi, Z. Wu, W. Zhu, L. Chen, X. Qiu, J. Phys. Chem. B 109 (2005) 20310–20314.
[9] D. Chen, M.A. Hickner, E. Agar, E.C. Kumbur, Electrochem. Commun. 26 (2013) 37–40.
[10] D. Xing, S. Zhang, C. Yin, B. Zhang, X. Jian, J. Memb. Sci. 354 (2010) 68–73.
[11] F. Zhang, H. Zhang, C. Qu, J. Phys. Chem. B 116 (2012) 9016–9022.
[12] H. Zhang, H. Zhang, X. Li, Z. Mai, W. Wei, Energy Environ. Sci. 5 (2012) 6299–6303.
[13] J. Qiu, M. Zhai, J. Chen, Y. Wang, J. Peng, L. Xu, J. Li, G. Wei, J. Membr. Sci. 342 (2009) 215–220.
[14] J. Ma, Y. Wang, J. Peng, J. Qiu, L. Xu, J. Li, M. Zhai, J. Membr. Sci. 419-420 (2012) 1–8.
[15] D. Chen, S. Kim, L. Li, G. Yang, M.A. Hickner, RSC Adv. 2 (2012) 8087–8094.
[16] K.W. Knehr, E. Agar, C.R. Dennison, A.R. Kalidindi, E.C. Kumbur, J. Electrochem. Soc. 59 (2012) A1446–A1459.
[17] K.W. Knehr, E.C. Kumbur, Electrochem. Commun. 23 (2012) 76–79.
[18] E. Agar, K.W. Knehr, D. Chen, M.A. Hickner, E.C. Kumbur, Electrochim. Acta 98 (2013) 66–74.
[19] X. Wei, L. Li, Q. Luo, Z. Nie, W. Wang, B. Li, G.-G. Xia, E. Miller, J. Chambers, Z. Yang, J. Power Sources 218 (2012) 39–45.
[20] C. Sun, J. Chen, H. Zhang, X. Han, Q. Luo, J. Power Sources 195 (2010) 890–897.
[21] K.W. Knehr, E.C. Kumbur, Electorchem. Commun 13 (2011) 342–345.
[22] DuPont. website: http://www2.dupont.com/FuelCells/en_US/products/literature.html (accessed 21.6.2011).
[23] D. Bernardi, M. Verbrugge, AIChE J 37 (1991) 1151–1163.
[24] J. Xi, Z. Wu, X. Teng, Y. Zhao, L. Chen, X. Qiu, J. Mater, Chem 18 (2008) 1232–1238.
[25] G. Pourcelly, A. Lindheimer, C. Gavach, J. Electroanal, Chem 305 (1991) 97–113.
[26] M. Verbrugge, R. Hill, J. Electrochem, Soc 137 (1990) 893–899.
[27] L. Yue, W. Li, F. Sun, L. Zhao, L. Xing, Carbon 48 (2010) 3079–3090.
[28] D. Aaron, Z. Tang, A.B. Papandrew, T.A. Zawodzinski, J. Appl, Electrochem 41 (2011) 1175–1182.
[29] E. Agar, C.R. Dennison, K.W. Knehr, E.C. Kumbur, J. Power Sources 225 (2013) 89–94.
[30] B. Schwenzer, J. Zhang, S. Kim, L. Li, J. Liu, Z. Yang, ChemSusChem 4 (2011) 1388–1406.
[31] M. Skyllas-Kazacos, M.H. Chakrabarti, S.A. Hajimolana, F.S. Mijalli, M. Saleem, J. Electrochem, Soc 158 (8) (2011) R55–R79.
[32] D.S. Aaron, Q. Lui, Z. Tang, G.M. Grim, A.B. Papandrew, A. Turhan, T.A. Zawodzinski, M.M. Mench, J. Power Sources 206 (2012) 450–453.
[33] M.P. Manahan, Q.H. Liu, M.L. Gross, M.M. Mench, J. Power Sources 222 (2013) 498–502.
[34] M.R. Hibbs, M.A. Hickner, T.M. Alam, S.K. McIntyre, C.H. Fujimoto, C.J. Cornelius, Chem. Mater 20 (2008) 2566–2573.
[35] M.A. Hickner, B. Pivovar, Fuel Cells 5 (2005) 213–229.